ACADEMIA ROMÂNĂ
Revue Roumaine de Chimie
http://web.icf.ro/rrch/

Rev. Roum. Chim.,
2012, *57*(4-5), 327-336

Dedicated to Professor Ionel Haiduc
on the occasion of his 75th anniversary

SYNTHESIS AND INVESTIGATION OF THE COPPER(II)-SUBSTITUTED POLYOXOTUNGSTATE BASED ON α-B-$[BiW_9O_{33}]^{9-}$ UNITS

Dan RUSU,[a,*] Adrian R. TOMŞA,[b] Graziella L. TURDEAN,[c] Ileana COJOCARU,[d] Oana BĂBAN[c] and Mariana RUSU[c,*]

[a] Faculty of Pharmacy, Iuliu Hatieganu University of Medicine and Pharmacy, 400023 Cluj-Napoca, Roumania
[b] Raluca Ripan Institute for Research in Chemistry, 400294 Cluj-Napoca, Roumania
[c] Faculty of Chemistry and Chemical Engineering, Babes-Bolyai University, 400056 Cluj-Napoca, Roumania
[d] Department of Horticulture, Craiova University, 200585 Craiova, Roumania

Received January 31, 2012

The new polyoxotungsto-bismutate, $Na_{12}[Cu_3^{2+}(H_2O)_3(BiW_9O_{33})_2] \cdot 47H_2O$ (**1**), has been synthesized by reaction of $Na_9[BiW_9O_{33}] \cdot 14H_2O$ and $Cu(CH_3COO)_2] \cdot H_2O$ in NaAc/HAc buffer under moderate condition. This polyoxoanion was characterized by elemental and thermo-gravimetric analysis, FT-IR, Raman, UV, Vis, EPR spectroscopy, X-ray diffraction on single crystal and cyclic voltammetry. This allowed for the subsequent determination of the behavior of the encapsulated transition metal ions, their coordination by the tungstobismutate (III) fragments, the corresponding local symmetry and the type of metal-metal interactions. Compound **1** consists of two α-B-$[BiW_9O_{33}]^{9-}$ units, which are linked by an equatorial belt of three $Cu(H_2O)^{2+}$ cations. Three $Na(H_2O)_2^+$ cations are also attached to the equatorial plane. The bond geometry is square-pyramidal against each Cu atom and trigonal-prismatic against each Na atom. Crystal data for **1** are: monoclinic, space group *C*2c, a=14.049(12) Å, b=23.360(19) Å, c=31.991(3) Å, α=90 °, β=99.217(2) °, γ=90 °, V=10364.2(15) Å^3, Z=4.

INTRODUCTION

The chemistry of polyoxometalates (POM) constitutes a large and rapidly expanding field of research. The increasing interest stems not only from fundamental considerations but also from their applications in material research, analysis, chemical catalysis and medicine.[1-3]

Lacunary polyoxometalates exhibit an increased reactivity towards transition metal ions, thus forming a broad variety of substituted polyoxometalates (TMSPs) in which the polyoxoanion framework remains unchanged or may rearrange in the course of the reaction with transition metal cations. It is well-known that the reaction of lacunary polyoxometalates α-B-$[XW_9O_{33}]^{9-}$, X=As^{III}, Sb^{III}, Bi^{III} with low-valent first-row transition metals usually leads to dimeric polyoxoanions with expected structures $[M^{n+}{}_3(H_2O)_3(\alpha\text{-B-}XW_9O_{33})_2]^{(18-3n)-}$.[4-24]

In this paper we report the synthesis and the physical properties of the new sandwich-type $Na_{12}[Cu^{2+}{}_3(H_2O)_3(BiW_9O_{33})_2] \cdot 47H_2O$ (**1**) polyoxo-tungsto-bismutate. In order to characterize this compound, the FT-IR, Raman, UV-VIS, EPR spectroscopy, single crystal X-ray diffraction, magnetic and electro-chemical measurements were performed.

* Corresponding authors: mrusu@chem.ubbcluj.ro or rdanrazvan@yahoo.com

RESULTS AND DISCUSSION

Synthesis and chemical analysis

The synthesis of the polyoxotungsto-bismutate $Na_{12}[Cu_3(H_2O)_3(BiW_9O_{33})_2]\cdot 47H_2O$(**1**) was made starting from **L** : Cu^{2+} (**L** = $Na_9[BiW_9O_{33}] \cdot 14\ H_2O$) in the molar rapport of 2:3 at a pH value of 4.7. Although under these circumstances most of the transitional metallic cations form Krebs compounds,[25] the case which we studied yielded a Hervé compound.[9] This can be explained on the basis that copper has the tendency to coordinate through five oxygen atoms in a C_{4v} symmetry.

The elemental analysis of the complex **1** is consistent with the proposed formula, i.e. $Na_{12}[Cu_3(H_2O)_3(BiW_9O_{33})_2]\cdot 47H_2O$.

X-Ray diffraction

Crystal data collection and refinement parameters for **1** are given in Table 1, and selected bond lengths and bonds angles of **1** are given in Table 2.

Table 1

Crystal Data and Structure Refinement for $Na_{12}[(Cu(OH_2))_3(BiW_9O_{33})_2]\cdot 47H_2O$ (**1**)

Formula	$Na_{12}[(Cu(OH_2))_3(BiW_9O_{33})_2]\cdot 47H_2O$	
Formula weight	6150.56	
Crystal system	Monoclinic	
Space-group	C2/c	
Unit cell dimensions	a=14.0496(12)Å	α= 90°
	b=23.3605(19)Å	β=99.217(2)°
	c= 31.991(3) Å	γ = 90°
V, Å^3	10364.2(15)	
Z	4	
Density (calculated), g cm^{-3}	3.942	
μ, mm^{-1}	24.051	
Radiation, wavelength, Å	Mo Kα, 0.71073	
Temperature, K	183(2)	
F_{000}	10980	
Crystal appearance	Green rhombus	
Crystal dimensions, mm	0.16 x 0.20 x 0.22	
Index ranges	-15<=h<=17, -22<=k<=29, -39<=l<=40	
Reflections collected	30024	
Independent reflections	11176	
R_{int}	0.0335	
Observed reflections [I> 2σ (I)]	10554	
Absorption correction	multi-scan	
Refinement method	Full-matrix least-squares on F^2	
R1 [I > 2σ (I)]	0.0474	
wR2 [I > 2σ (I)]	0.1204	
R1 (all data)	0.0501	
wR2 (all data)	0.1219	
GOF on F^2	1.22	
$\Delta\rho_{max,min}$/e Å^{-3}	3.425 and -5.146	

Table 2

Selected Bond Lengths (Å) and Angles (deg) for $Na_{12}[(Cu(OH_2))_3(BiW_9O_{33})_2]\cdot 47H_2O$ (**1**)

W-O_t[a]	1.718(9) – 1.749(9)
Bi-$O_{(BiW3)}$[b]	2.096(8) - 2.116(8)
W-$O_{(BiW3)}$[b]	2.213(8) - 2.299(9)
W-$O_{(W2)}$[b]	1.885(8) - 2.016(9)
W-$O_{(CuNaW)}$[b]	1.801(9) – 1.822(9)
Cu-$O_{(CuNaW)}$[b]	1.905(9) – 1.953(8)
Cu-$O_{(CuH2)}$[b]	2.192(13) – 2.278(9)
$NaO_{(CuNaW)}$[b,c]	2.470(10) - 2.536(9)
Na-$O_{(CuH2)}$[b,c]	2.375(12) - 2.879(8)
O-Bi-O	86.7(3) - 87.6(3)

Table 2 (continued)

O-W-O $_{trans}$	157.1(4) - 170.7(4)
O-W-O $_{cis}$	72.9(3)-104.7(4)
O-Cu-O $_{cis}$	87.3(4) - 101.7(3)
O-Cu-O $_{trans}$	156.7(5) - 168.0(4)

[a] t indicates a terminal oxygen. [b]The subscript letters indicate symbol and numbers of bonded neighbor atoms of oxygen. [c]Na refers to Na atoms in the Cu_3Na_3 belt.

The copper complex **1** crystallizes in the monoclinic space group C2/c, with a total number of 52 atoms in the anion part containing 9W (W1–W9), 1Bi (Bi), 2Cu (Cu1-Cu2), 33O (O1–O33), 2Na (Na1-Na2) and 5H2O (O34, O35, O41, O44, O46) atoms. The anion structure of $[(Cu(OH_2))_3(BiW_9O_{33})_2]^{12-}$ **1a** consist of two lacunary α- B- $[BiW_9O_{33}]^{9-}$ Keggin moieties which are linked by O-Cu-O bridges into an assembly of virtual D_{3h} symmetry (Fig. 1). Each Cu, in the equatorial plane of the anion, shares an oxygen with each of the two W atoms in an edge-sharing pair of WO_6 octahedra in each α-B-$[BiW_9O_{33}]^{9-}$ unit. An apical water molecule completes each square-pyramidal CuO_5 group. In addition, three Na atoms lie in the equatorial plane. Each Na is linked to two Cu-bonded oxygens of each of the W atoms in a corner-sharing pair of octahedra in each α-B-$[BiW_9O_{33}]^{9-}$ unit, and is also bonded to two H_2O ligands which complete a distorted trigonal-prismatic NaO_6 group. Thus, the anion **1a** could be formulated $[\{Cu(H_2O)\}_3\{Na(H_2O)_2\}_3(BiW_9O_{33})_2]^{9-}$.

Comparison of the independent Cu···Cu distances [4.835, 4.919 Å] with the Na···Na distances [6.662, 6.704 Å] shows that the Na atoms lie distinctly further from the anion axis, which is in agreement with the small displacement of the Cu atoms from the basal planes of the CuO_5 of the square–pyramidal groups. These displacements are in the range of the displacements of the Cu in previously published compound [0.3191, 0.2673 and 0.2673 Å compared to 0.24, 0.30, 0.30(1) Å] [4] and smaller than corresponding displacements of the vanadium atoms [0.57–0.61(1) Å].[7]

The structure of the anion is closely similar to that of previously published $[(VO)_3(\alpha\text{-}BiW_9O_{33})_2]^{12-}$ [7] and $[\{Cu(H_2O)\}_3\{Na(H_2O)_2\}_3(BiW_9O_{33})_2]^{9-}$,[14] although the Bi···Bi distance is slightly longer [4.567 Å compared with 4.504(1) Å and 4.549 Å, respectively]. The small O–Bi–O angles [86.668(3)-87.596(3)] are in the same range observed in other tungstobismuthate polyanions.[25] The Bi–O bond lengths are not significantly different from those in the previously published compounds (2.09–2.11(1) Å in the V compound; and 2.08(2)–2.13(2) Å in the Cu compound. Anion is closely resembles the structure of several related anions of the type $[\{M(H_2O)\}_3(\alpha\text{-}B\text{-}XW_9O_{33})_2]^{n-}$ (where M(II) = Mn, Co, Cu, Zn; X(III) = As, Sb; X(IV) = Se, Te).[4-5, 9-10]

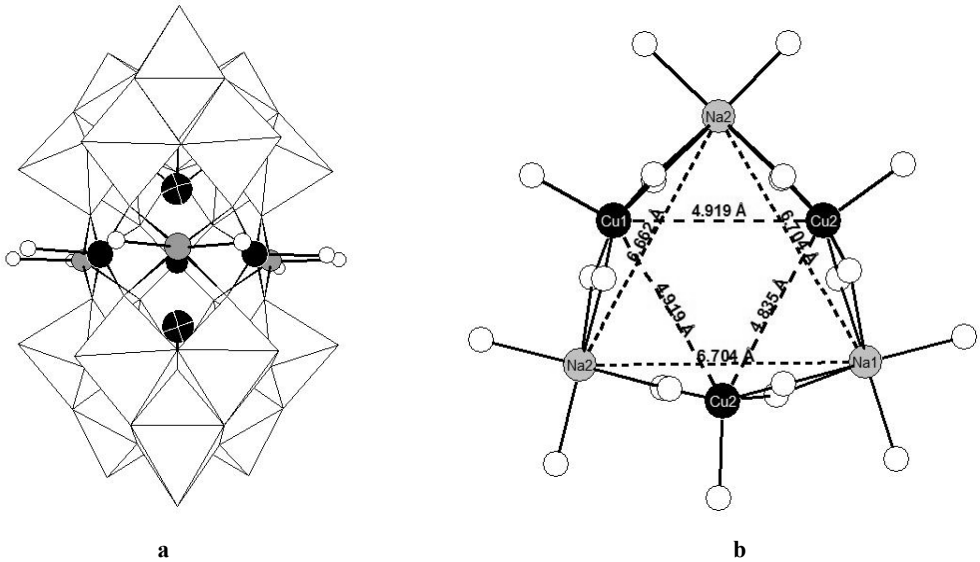

a **b**

Fig. 1 – (a) Combination of ball-and-stick / polyhedral representation of $[\{Cu(H_2O)\}_3\{Na(H_2O)_2\}_3(BiW_9O_{33})_2]^{9-}$ **(1a)**. The coordination geometry of Cu (black spheres), Na (gray spheres), and Bi (crosshatched black spheres) is clearly visible. Oxygen atoms and water molecules are represented as small white spheres. (b) The relevant distances for equatorial belt arrangement.

Thermal stability

The thermal stability of 1 was investigated by TG-DTG-DTA. The weight loss in the 25 – 500 °C range corresponds to 32 water molecules. The loss of water by heating proceeds in three steps, as observed on the DTG curve. In the first step, 25 – 300 °C the lattice water molecules are lost (29 water molecules), while the loss of the water coordinated to Cu^{2+} ions proceeds in the next two steps (2 water molecules between 300 – 400 °C, and one water molecule between 400 – 500 °C). The dehydration process is accompanied by an endothermic process between ~ 25 – 200 °C, as observed on the DTA curve (Fig. 2).

According to the literature, the first exothermic peak of DTA curve is regarded as the thermal stability sign of polyoxometallate.[26, 27] For **1**, the first exothermic peak appeared at 398°C, indicating a good thermal stability of the complex. The second exothermic peak at 561°C may be assigned to some phase transitions of the resulting oxides.

Electronic spectra

UV electronic spectrum of **1** contains two bands characteristic for metal charge transfer in the heteropolyoxometalate frame. The more intense band corresponding to the $p_\pi(O_t) \rightarrow d_{\pi^*}(W)$ transitions,[28] is centered at 193.6 nm. The broader band centered at 254.1 nm in the complex spectrum belongs to the $p_\pi(O_{c,e}) \rightarrow d_{\pi^*}(W)$ charge transfer transition in the tricentric bonds.[29]

Vis-NIR spectrum. Information about the local environment of $3d^9$ metal ions in the **1** has been obtained by means of d-d transitions from the visible electronic spectra performed in aqueous solutions. The visible spectrum of complex **1** has been interpreted in terms of five-coordination of every copper cation and a distorted square-pyramidal local symmetry.

The very broad band at 824 nm in the visible electronic spectrum of the complex **1** was assigned to the $B_1(d_{x^2-y^2}) \rightarrow E(d_{xz,yz})$ transitions for the Cu^{II} ions in C_{4v} local symmetry. Three transitions are expected ($d_{xy}, d_{yz} \rightarrow d_{x^2}$ and $d_{xy} \rightarrow d_{x^2-y^2}$) but these are very close in energy and give rise to a single broad band.[30]

Vibrational spectra

FT-IR spectra of compound **1** and of the ligand **L** polyoxometalate are displayed in Fig. 3 and are quite similar, suggesting that two polyoxometalates belong to the same series. The stretching vibration of the terminal $W=O_t$ bonds is recorded at about 940 cm^{-1} for both polyoxometalates. This indicates that the terminal oxygen atoms are not involved in the coordination of Cu^{2+} metal centers.

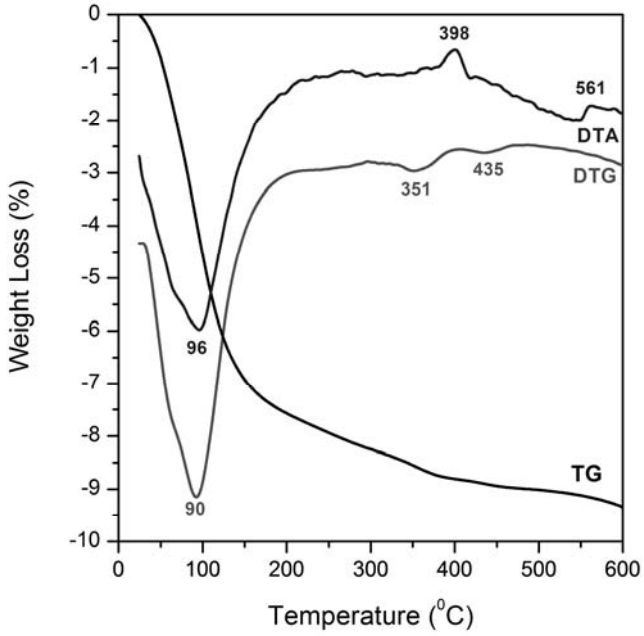

Fig. 2 – Thermogravimetric and thermodifferential curves of the $Na_{12}[Cu_3^{2+}(H_2O)_3(BiW_9O_{33})_2] \cdot 47H_2O$ (**1**) complex.

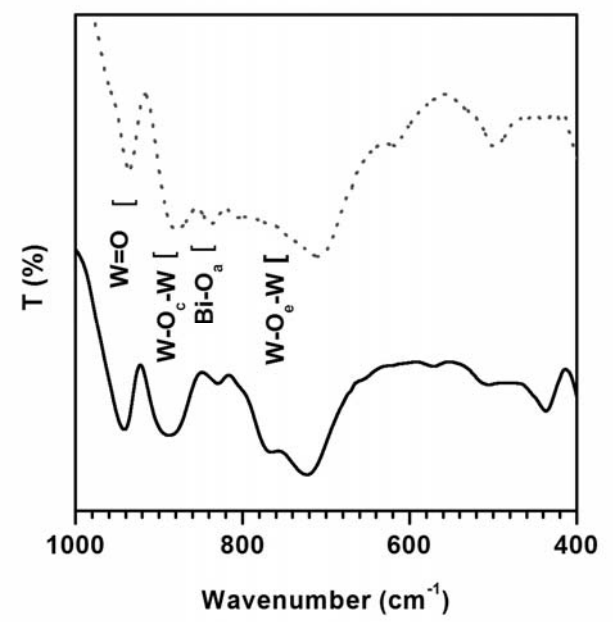

Fig. 3 – FT-IR spectra of the $Na_{12}[Cu_3^{2+}(H_2O)_3(BiW_9O_{33})_2]\cdot 47H_2O$ (**1**) (——) and $Na_9[BiW_9O_{33}]\cdot 14H_2O$ (**L**) (·····) recorded in KBr pellets.

The main stretching vibration of the Bi-O_i bonds is recorded at around 830 cm^{-1} for both substances. This shows that internal oxygen is not involved in the coordination of Cu^{2+}.

The vibrational of tricentric W-O_c-W bonds of the corner sharing WO_6 octahedra are recorded at 888 and 768 for **1** 879 and 807 cm^{-1} for **L**, respectively. The two peaks demonstrated the non equivalence of W-O_c-W bonds when linking octahedra from equatorial and polar regions of the trilacunary fragments. [31]

The vibration bands of tricentric W-O_e-W bonds of the edge–sharing WO_6 octahedra are also split, being revealed at 723 and 571 cm^{-1} for **1** and at 710 and 500 cm^{-1} for **L**, respectively. The splitting evinces the presence of two non-equivalent bonds of this type in the oxo-cage. As expected, spectrum **1** displays a broad band, due to the new metal centers. This maximum is recorded at 437 cm^{-1} and can be attributed to the stretching vibration ν_{as}Cu-O superimposed over ν_{as}Bi-O_i.

Raman spectrum of polyoxometalate **1** shows characteristic strong vibration bands at 968, 960 and 214 cm^{-1}, which are assigned to the ν_s(W-O_t), ν_{as}(W-O_t) and ν_s(W-O_i), vibrations, respectively, where O_t represents terminal oxygen and O_i represents the bridging oxygen between the internal bismuth heteroatom and tungsten addenda.[31]

EPR spectrum

The shape of the powder EPR spectrum of the complex **1** (Fig. 4) obtained in the X-band at room temperature is similar to the one which was previously reported for the Cu^{II} trinuclear cluster encapsulated in As^{III} heteropolyanion.[9, 32]

The antiferromagnetic coupling between the Cu^{II} ions, favorised by the geometry of the cluster and the spin frustration, leads to a double degenerate S = 1/2 ground state, which is EPR inactive, and one EPR active S = 3/2 excited state. The best fit of the spectrum was obtained with an axial spin Hamiltonian of S = 3/2, and principal g values, $g_1 = g_{II} = 2.075$ and $g_2 = g_\perp = 2.240$, the axial zero field splitting parameter D = 0.0214 cm^{-1} and the linewidths ΔB_{II} = 106 G, $\Delta B_\perp$ = 68 G were obtained. The parallel direction is along the C_3 axis of the trinuclear copper cluster and also along the perpendicular direction of the individual g tensors.

The powder EPR spectrum of complex **1** at room temperature can be interpreted by spin Hamiltonian.[32] This behavior is in agreement with the antiferromagnetic coupling and the spin frustration lead to an S = 1/2 EPR inactive ground state.

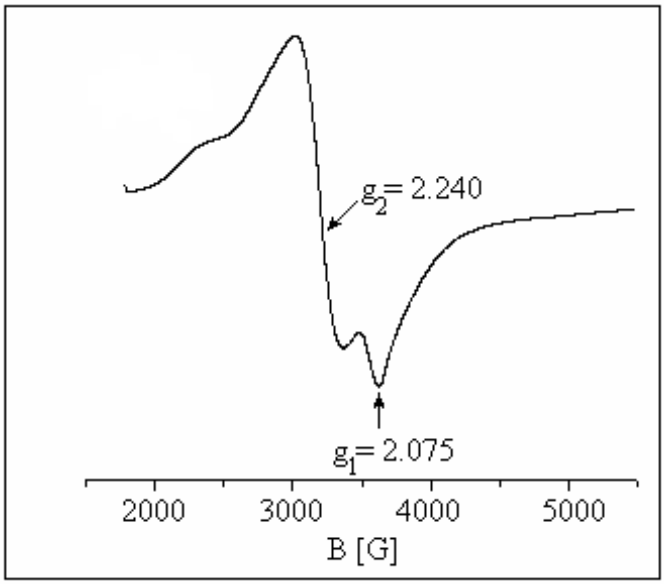

Fig. 4 – The experimental power EPR spectrum of $Na_{12}[Cu_3^{2+}(H_2O)_3(BiW_9O_{33})_2]\cdot 47H_2O$ (**1**) obtained in X-band at room temperature.

Cyclic voltammetry

The electrochemical behavior of the **1**, investigated by cyclic voltammetry, is presented in Fig. 5. The voltammograms reveals the appearance of waves corresponding to the redox behavior of Cu(II) $\rightarrow$Cu(I) $\rightarrow$Cu(0) (wave I_a/I_c) and to the reduction of W(VI) $\rightarrow$ W(V) (wave II_c, III_c). Also, it is visible a split of peak I_a do to the redox behavior of the Bi ion (peak I_a', inset of figure 1), which shift from the 0 V *vs*. Ag/AgCl, KCl_{sat} in the $Bi(NO)_3$ to a potential of -0.150 V *vs.* Ag/AgCl, KCl_{sat} in the compound **1**. This behavior is superposed on the redox behavior of Cu, taking place at +0.05 V *vs.* Ag/AgCl, KCl_{sat}.

In order to identify the contribution of the Cu^{2+} ions and Bi^{3+} respectively, on the redox response of complex **1**, increasing volumes of 1 mM $CuSO_4$ and 1 mM $Bi(NO_3)_3$ were added to a 1 mM compound **1** solution, and the corresponding cyclic voltammograms were recorded (Fig. 5, respectively the inset of Fig. 5).

As shown from Fig. 5, the addition of $CuSO_4$ leads to a significant increase in the Ia peak current, while the other peaks (Ic, IIc and IIIc) remain practically unchanged. Further, the addition of Bi^{3+} ions in the compound **1** solution does not change its voltammetric response (inset of Fig. 5).

The electrochemical parameters (ΔEp and Ipa/Ipc) of the peaks, corresponding to **1**, indicate a quasi-reversible (peak I) or irreversible (peak II and III) redox processes for freely diffusing redox couples. [33]

The influence of the scan rate on the redox behavior of compound **1** is shown in Fig. 6.

It is worth mentioning that the slopes of the log–log dependence between the peak currents and the potential scan rate for the peaks of complex **1** (results not shown) are equal to 0.5 for anodic peak (R = 0.9957, n = 10) and 0.9 for the cathodic peak (R = 0.9944, n = 10) revealing that the absorption of the complex on the electrode surface during the cathodic scanning is not negligible. Thus, this behavior indicate that the redox processes involved in the electrochemical activity of **1** are mixed, being both diffusion- and surface-controlled.[34]

Generally, the reduction of the polyoxometallates is accompanied by protonation, therefore, the pH of the solution has a great effect on the electrochemical behavior of the polyoxometalates.

The effect of the pH on the redox behavior of complex **1** was also investigated. Fig.7 illustrates the cyclic voltammograms recorded at pH between 3.25 - 6.

In our case, for peak I_a a slight shift of the redox potentials to negative values is observed at higher pH. This is a common behavior in polyoxometalate complexes, where the uptake of protons during reduction of the complex is to avoid charge concentration on the polyoxometalate (accumulation of electrons).[34]

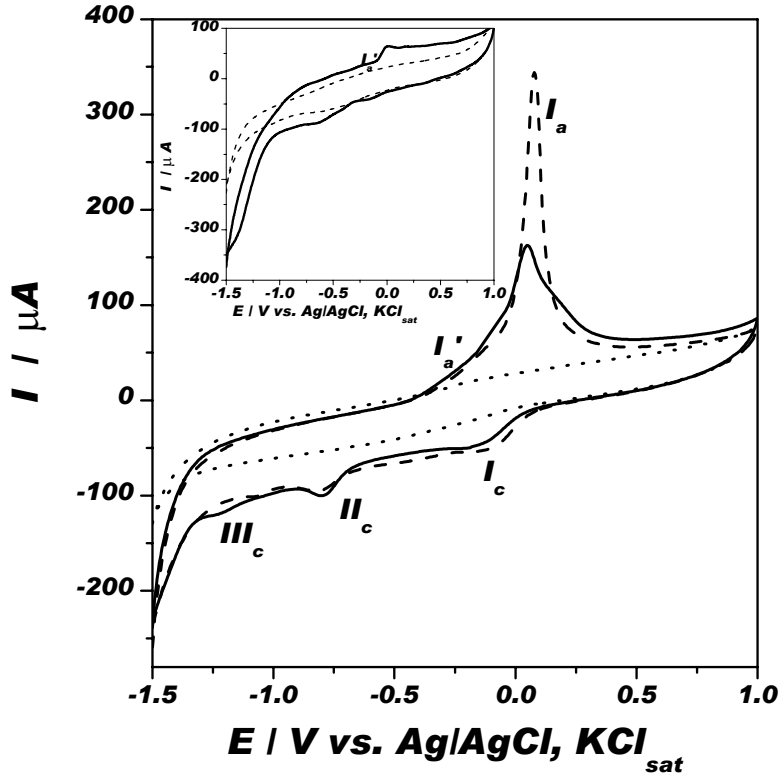

Fig. 5 – Voltammetric response of 10^{-3}M $Na_{12}[Cu_3^{2+}(H_2O)_3(BiW_9O_{33})_2]\cdot 47H_2O$ (**1**) (solid line) and in the presence of 10^{-3} M $CuSO_4$ (dash line) on graphite electrode. Inset: Voltametric response of 10^{-3} M $Bi(NO)_3$ (solid line) on the graphite electrode. Experimental conditions: electrolyte, Na_2SO_4 0.25 M, pH 5.1 (dot line), scan rate, 50 mV*s^{-1}; starting potential, -1.5 V vs. Ag/AgCl, KCl_{sat}

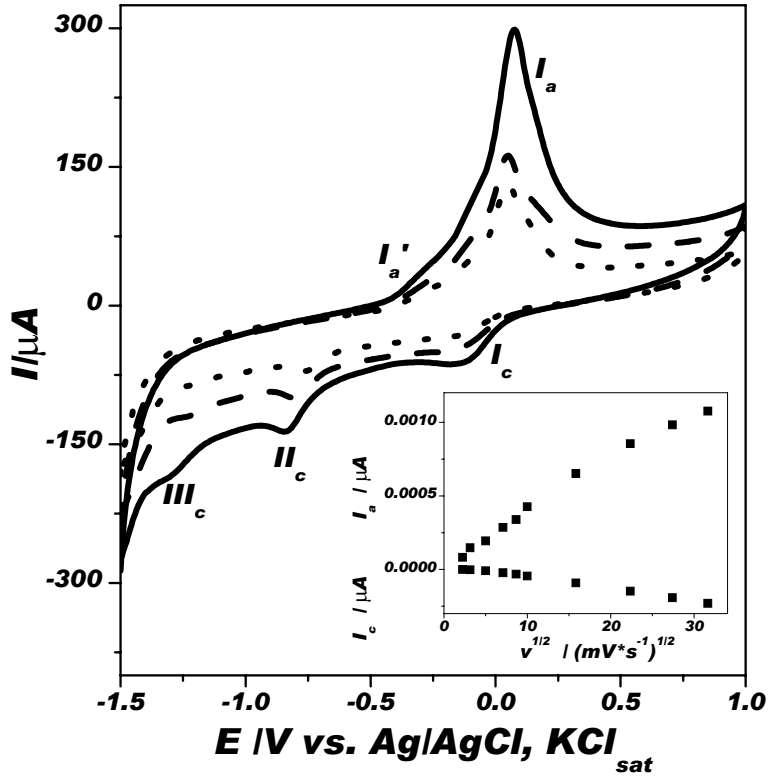

Fig. 6 – Voltammetric response of 10^{-3}M $Na_{12}[Cu_3^{2+}(H_2O)_3(BiW_9O_{33})_2]\cdot 47H_2O$ (**1**) on graphite electrode at different scan rate and I *vs.* $v^{1/2}$ dependence (inset). Experimental conditions: electrolyte, Na_2SO_4 0.25 M, pH 5.1, scan rate, 25 mV*s^{-1} (dot line), 50 mV*s^{-1} (dash line), 100 mV*s^{-1} (solid line); starting potential, -1.5 V vs. Ag/AgCl, KCl_{sat}.

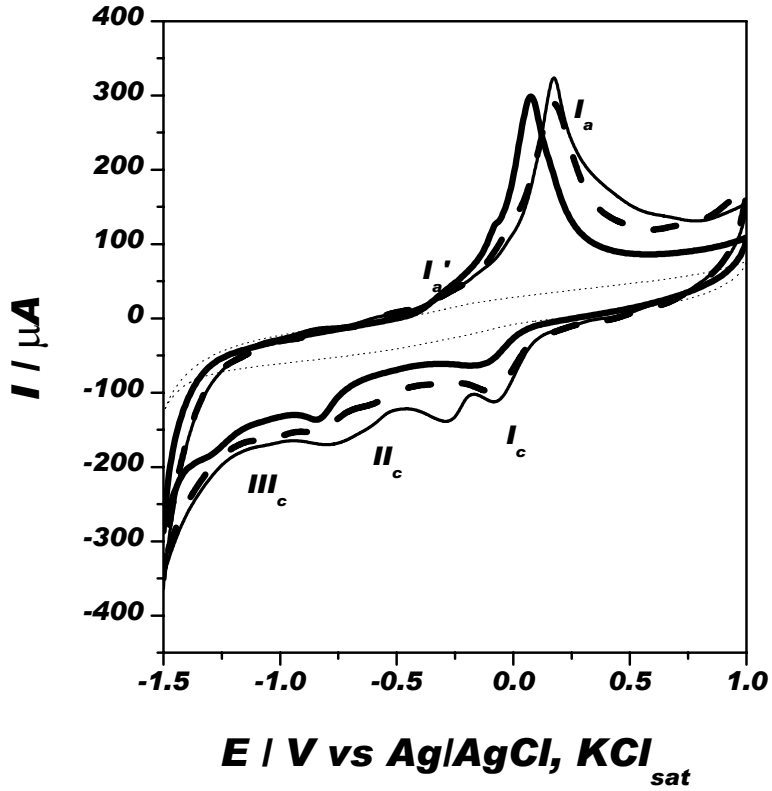

Fig. 7 – Cyclic voltammograms of 10^{-3}M $Na_{12}[Cu_3^{2+}(H_2O)_3(BiW_9O_{33})_2]\cdot 47H_2O$ (**1**) on graphite electrode at pH 6 (solid line), pH 4.65 (dash line), pH 3.25 (solid thin line). Experimental conditions:electrolyte, Na_2SO_4 0.25 M, pH 5.1 (dot line), scan rate, 100 $mV*s^{-1}$; starting potential, -1.5 V vs. Ag/AgCl, KCl_{sat}.

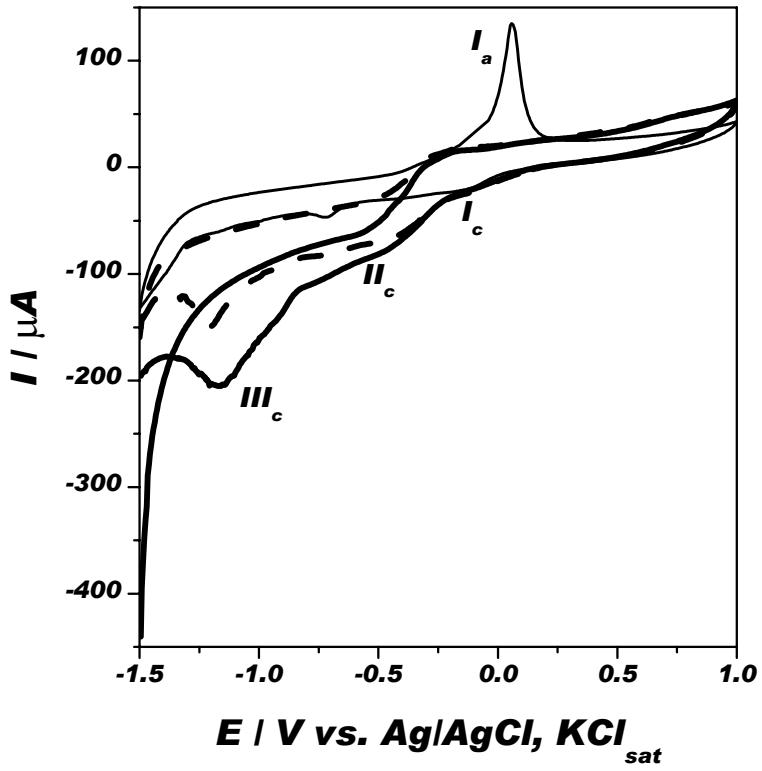

Fig. 8 – The electrocatalytic effect of 10^{-3}M $Na_{12}[Cu_3^{2+}(H_2O)_3(BiW_9O_{33})_2]\cdot 47H_2O$ (**1**) (solid thin line) on 0.02 M (dash line) and 0.04 M (solid line) H_2O_2 electroreduction at graphite electrode. Experimental conditions: electrolyte, Na_2SO_4 0.25 M, pH 5.1, scan rate, 25 $mV*s^{-1}$; starting potential, -1.5 V vs. Ag/AgCl, KCl_{sat}.

The mediated electroreduction of H_2O_2 is of general interest for many practical applications, such as biosensors and fuel cells.[35, 36] While the H_2O_2 reduction on conventional electrodes requires large over-potentials,[37, 38] it was reported that the electroreduction of H_2O_2 can be activated by polyoxometalates.[39] Being readily reduced at quite positive potentials, these complexes serve as powerful electron reservoirs.[40] The electrocatalytic activity on the H_2O_2 reduction in the presence of compound **1** at a graphite electrode is presented in Fig. 8.

The electrocatalysis occurs at peaks II_c and III_c; the intensity of these peak currents increase with the increase of the H_2O_2 concentration, while the intensity of peak I_c is unaffected by the presence of H_2O_2.

EXPERIMENTAL

Materials

All chemicals purchased were of reagent grade and used without further purification.

The trilacunary polyoxometalate $Na_9[BiW_9O_{33}]\cdot 14H_2O$ (**L**) was prepared according to the published method.[3] The identity of the precursor was established by FT-IR spectra (cm^{-1}, KBr pellets, polyoxometalate region): 938 (s), 879 (vs), 838 (vs), 807 (s), 710 (vs), 500 (m), 436 (m), and UV (H_2O, λ nm/cm^{-1}): 194/51426; 254/39231.

Synthesis of $Na_{12}[Cu^{2+}{}_3(H_2O)_3(BiW_9O_{33})_2]\cdot 47H_2O$ (1)

An amount of 0.60 g (3 mmol) of $Cu(CH_3COO)_2.H_2O$ was dissolved in 60 ml of molar CH_3COONa/CH_3COOH buffer (pH=4.7), and 5.7 g (2 mmol) of $Na_9[BiW_9O_{33}]\cdot 14H_2O$ as ligand (L) was added while stirring. The mixture was heated at 60°C for 1 hour while the color changed from green to yellow-green. The resulting solution was filtered through a medium frit and allowed to cool to room temperature. After 6 days micro-crystals were obtained by filtration and washed with NaCl (2M), ethanol and diethyl ether and dried in air. Yield: 5 g (82% based on W). Calcd. For $Na_{12}Bi_2W_{18}Cu_3O_{116}H_{100}$: Na 4.48, Cu 3.10, Bi 6.79, W 53.80. Found: Na 4.24, Cu 3.04, Bi 6.82, W 53.75. FT-IR (cm^{-1}, KBr pellets, polyoxometalate region): 941 (s)-ν_{as}(W-O_t), 888 (s,br)- ν_{as}(W-O_c-W), 829 (w) - ν_{as}(Bi-O_i), 768 (vs) ν_{as}(W-O_e-W), 723 (vs,b) ν_s(W-O_e-W),, 571 (w), 511 (m) δ(W-O-W), 437 (m,sp) ν_{as}(Bi-O_i + Cu-O). Raman (cm^{-1}): 968-ν_s(W-O_t), 960-ν_{as}(W-O_t), and 214-ν_s(W-O_i). UV-Vis (H_2O, λ nm/cm^{-1}): 193.6/51652; 254.1/39354; 824/12135.

The complex **1** was allowed to crystallize after dissolution in a minimum amount of hot water. After a few days the crystals were collected.

Analysis

Elemental analysis was performed by inductively coupled plasma atomic emission spectroscopy on an ICP-OES Perkin Elmer Optima 3500 DV spectrometer. The water content was determined thermo-gravimetrically, with a METTLER-TOLEDO TG/SDTA 851 thermo-gravimeter (Pt crucible, 20 mL/min nitrogen flow, 5 ºC/min heating rate).

Investigations

FTIR spectra were recorded on a Jasco FT/IR 615 spectrophotometer, in the 4000-400 cm^{-1} range, using KBr pellets.

Raman spectra were registered on a Bruker FRIR IFS 66, with a Ramab FRA 106 unit spectrophotometer (λ_e = 1064 nm), using KBr pellets.

UV and visible electronic spectra were recorded in the λ=190-900 nm range in aqueous solution (5.10^{-5}M–5.10^{-3}M), using a standard UV-Vis JASCO V-670 spectrophotometer.

EPR spectra on powdered solids were recorded at room temperature (9.40 GHz) in the X-band using a JOEL-JES-3B spectrometer. All g values have been estimated with a ± 0.002 precision.

The cyclic voltammetry was carried out using a computer-controlled electrochemical analyzer (PGStat 10, AutoLab, Nederlands). All electrochemical studies were performed at room temperature, using a conventional three cell with a graphite working electrode (Ringsdorff, Germany), a platinum wire auxiliary electrode and an Ag/AgCl, KCl_{sat} reference electrode, respectively. Before use, the working electrode was cleaned by polishing with successively finer grade emery paper. The compound 1 solution was freshly prepared just before use, by dissolving the appropriate amounts of complex into the supporting electrolyte. The supporting electrolyte was 0.25 M solution of Na_2SO_4, prepared from the corresponding salts provided of Merck (Darmstadt, Germany). The pH values of the solutions were adjusted using diluted sulphuric acid (the reactive used was from Bucharest, Roumania).

Crystals of **1** were removed from the mother liquor and immediately cooled to 183(2) K on a Bruker AXS SMART diffractometer (three circle goniometer with 1K CCD detector, Mo-Kα radiation, graphite monochromator (λ = 0.71073 Å); hemisphere data collection in ω at 0.3° scan width in three runs with 606, 435 and 230 frames (φ = 0, 88 and 180 °) at a detector distance of 5 cm). A total of 30024 reflections ($1.71 < \theta < 27.00°$) were collected of which 11176 reflections were unique (R_{int}= 0.0335). An empirical absorption correction using equivalent reflections was performed with the SADABS 2.03 software. The structure was solved with the SHELXS-97 software and refined using SHELXL-97 software to R = 0.0474 for 10554 reflections with $I > 2\sigma(I)$, R = 0.0501 for all reflections; Max/min residual electron density 3.425 and -5.146 e Å^{-3}. (SHELXS/L, SADABS from G.M. Sheldrick, University of Göttingen 1997/2001; structure graphics with DIAMOND 2.1 from K.Brandenburg, Crystal Impact GbR, 2001).

Further details of the crystal structure determination may be obtained from the Fachinformationszentrum Karlsruhe, 76344 Eggenstein-Leopoldshafen, Germany (fax: (+49)7247-808-666; e-mail: crysdata@fiz-karlsruhe.de) on quoting the depository no. CSD 420625.

CONCLUSIONS

The chemical and thermo-gravimetric analysis confirm the proposed molecular formula for complex **1** $Na_{12}[Cu_3{}^{2+}(H_2O)_3(BiW_9O_{33})_2]\cdot 47H_2O$ in good agreement with X-ray diffraction data. The difference between the number of crystallisation

water molecules determined by the crystallographic and thermo-gravimetric data is owed to the different hydration of the samples that were subject to these measurements. The acidity of the reaction medium (pH=4.7) and the preferred coordination geometry of the incorporated copper cations are significantly for obtained complex **1**.

The spectroscopic investigations of **1**, as well as X-ray diffraction analysis confirm the sandwich-type structure of this compound and the encapsulation of the trinuclear copper metal cluster between two trivacant Keggin units. Copper cations are penta-co-ordinate in square-pyramidal environments and the local symmetry is C_{4v}. The geometry of the triangular cluster Cu_3 and the spin frustation favours the antiferromagnetic interactions.

The preliminary electrochemical studies (scan rate and pH influence) of the new compound **1** have exhibited a quasi-reversible (peak I_a/I_c) and irreversible (peaks II_c, III_c) behavior. The redox processes at peak I are mixed ones, being both diffusion- and surface-controlled and sensitive at the pH of solution. The electrocatalytic activity of the compound **1** towards H_2O_2 was also evidenced.

Acknowledgments: The authors express their gratitude towards the Chemistry Department of Bielefeld University from Germany for allowing the use of the X-ray diffractometer and especially towards Dr. Alice Merca for collecting the crystallographic data.

REFERENCES

1. M.T. Pope and A. Müller, Angew. *Chem. Int. Edit,* **1991**, *30*, 34-48.
2. J.T. Ruhle, C.L. Hill, D.A. Judd and R.F. Schinazi, *Chem. Rev.,* **1998**, *98*, 327-357.
3. B. Krebs and R. Klein in "Polyoxometalates: from Platonic Solids to Anti-Retroviral Activity", (eds. M.T. Pope and A. Müller), Kluwer Academic Publishers, Dordrecht, Boston, London, 1994, p. 41-57.
4. F. Robert, M. Leyrie and G. Hervé, *Acta Crystallogr. Sect. B*, **1982**, *38*, 358-362.
5. M. Bösing, A. Nöh, I. Loose and B. Krebs, *J. Am. Chem. Soc*., **1998**, 120, 7252-7259.
6. D. Rusu, C. Rosu, M. Rusu and G. Marcu, *Stud. Univ. Babes-Bolyai, Chem*., **2000**, *45*, 139-146.
7. B. Botar, T. Yamase and E. Ishikawa, *Inorg. Chem. Commun.,* **2001**, *4*, 551-554.
8. T. Yamase, B. Botar and E. Ishikawa, *Chem.Lett.,* **2001**, 56-57.
9. P. Mialane, J. Marriot, E. Rivière, J. Nebout and G. Hervé, *Inorg. Chem*., **2001**, *40*, 44-48.
10. U. Kortz, N.K. Al-Kassen, M.G. Saveliejj, N.A. Al Kadi and M. Sadakane, *Inorg. Chem*., **2001**, *40*, 4742-4749.
11. G. Sazani, M.H. Dickman and M.T. Pope, *Inorg. Chem.,* **2001**, *39*, 939-943.
12. D. Rusu, C. Craciun, Anne-Laure Barra, L. David, Rusu, C. Rosu, O. Cozar and G. Marcu, *J. Chem. Soc. Dalton Trans,* **2001**, 2879-2887.
13. D. Rusu, C. Rosu, C. Craciun, L. David, M. Rusu and G. Marcu, *J. Molec. Struct*., **2001**, *563-564*, 427-433.
14. C. Rosu, D. Rasu and T.J.R. Weakley, *J.Chem. Cryst.*, **2003**, *33*, 751-755.
15. T. Yamase, E. Ishikawa, K. Fukaya, H. Nojiri, T. Taniguchi and T. Atake, *Inorg. Chem*., **2004**, *43*, 8150-8157.
16. O. Serdan, D. Rusu, P. Ilea and I.C. Popescu, *Rev. Roum. Chim,* **2004**, *49*, 465-474.
17. D. Rusu, C. Craciun, M. Rusu and L. David, *Rev. Roum. Chim*., **2005**, *50*, 87-96.
18. R. Copping, I. May, D. Collison, C.J. Jones, C.A. Sharrad and M.J. Sarsfield, *Royal Soc. Chem,*. **2006**, 305, 243-245.
19. R. Copping, A.J. Gaunt, I. May, C.A. Sharrad, D. Collison, M. Helliwel, F.O. Fo and C.J. Jones, *Chem. Commun,* **2006**, *36*, 3788-3790.
20. C-Y. Sun, S-X. Liu, C-L. Wang , L-H. Xie, C-D. Zhang, B. Gao and E-B. Wang, *J. Coord. Chem.*, **2007**, *60*, 567-579.
21. H. Tan, Z. Zhang, D. Liu, Y. Qi, E. Wang and Y. Li, J. *Clust. Sci,* **2008**, *19*, 543-550.
22. M.H. Alizadeh and M. Mohadeszadeh, *J. Clust. Sci.,* **2008**, *19*, 435-443.
23. Z-H. Xu, J. Liu, E-B. Wang, C. Qin, Q. Wu and Q. Shi, *J. Molec. Struct*., **2008**, *873*, 41-45.
24. H. Liu, Y. Liu, H. Liu, C. Shi, F. Liu and H. Liu, *Inorg. Chem. Commun.,* **2009**, *12*, 1-3.
25. I. Loose, E. Droste, M. Bösing, H. Pohlmann, M. Dickman, C. Rosu, M.T. Pope and B. Krebs, *Inorg. Chem.*, **1999**, *38*, 2688-2694.
26. Q. Wu, E. Wang and J. Liu, *Polyhedron,* **1993**, *12*, 2563-2569.
27. G. Sun, J. Feng, H. Wu, F. Pei, K. Fang and H. Lei, *J. Magn. Mater*., **2004**, *281*, 405- 411.
28. T. Yamase, *Chem. Rev*., **1998**, *98*, 307-325.
29. H. So and M.T. Pope, *Inorg. Chem*., **1972**, *11*, 1441-1448.
30. B.J. Hathaway, "Comprehensive Coordination Chemistry", Pergamon Press, Oxford, 1987, p. 59.
31. C. Rocchiccioli-Deltcheff, M. Fournier, R. Franck and R. Thouvenot, *Inorg. Chem*., **1983**, *22*, 207-211.
32. Y.H. Cho and H. So, *Bull. Korean Chem. Soc.,* **1995**, *16*, 243-249.
33. A.J. Bard and L.R. Faulkner, "Electrochemical Methods", Wiley-VCH, New York, 1980, p. 522-525.
34. M. Ammam, B. Keita, L. Nadjo and J. Fransaer, *Talanta*, **2010**, 2132-2140.
35. L. Bi, J. Liu, Y. Shen, J. Junguang and S. Dong, *New J Chem*., **2003**, *27*, 756-764.
36. D. Martel and A. Kuhn, *Electrochim. Acta,* **2000**, *45*, 1829-1836.
37. Z. Han, Y. Zhao, J. Peng, A. Tian, Y. Feng and Q. Liu, *J. Solid State Chem.*, **2005**, *178*, 1386-1394.
38. X. Wang, H. Zhang, E. Wang, Z. Han and C. Hu, *Mater. Lett.* **2004**, *58*, 1661-1664.
39. K. Foster, L. Bi and T. McCormac, *Electrochim. Acta*, **2008**, *54*, 868-875.
40. W. Song, X. Wang, Y. Liu, J. Liu and H. Xu, *J. Electroanal. Chem*., **1999**, *476*, 85-89.